Lymphology 20 (1987) 25-35

PULMONARY CIRCULATION, EXTRAVASCULAR WATER, AND SOLUTE FLUX AS DETERMINED BY POSITRON EMISSION TOMOGRAPHY

D.P. Schuster, M.A. Mintun

Department of Internal Medicine (Respiratory and Critical Care) and Division of Radiation Science, Mallinckrodt Institute of Radiology, Washington University Medical School, St. Louis, Missouri

ABSTRACT

Pulmonary edema is the result of an increased transpulmonary flux of water and solute and a concomitant insufficiency of lung lymphatic drainage. Although this pathogenetic concept seems well-established, the microcirculatory details of pulmonary edema formation and its ultimate resolution are still poorly understood. For example, how do regional changes in pulmonary blood flow affect the resolution of pulmonary edema, and in turn, how do they affect pulmonary gas exchange? When does vascular permeability return to normal after acute lung injury? Is the severity of the permeability defect related to prognosis, and can therapy hasten either the resolution of altered permeability or the accumulation of extravascular lung water? These and similar questions are approachable with positron emission tomography (PET) and are outlined in this brief review.

INTRODUCTION

Technological limitations have often been a major impediment to the study of acute respiratory failure. Radiopharmaceuticals and external radiation counting techniques have often been useful, but the inability to make accurate, quantitative regional measurements in the presence of significant lung disease has hampered progress. The development of positron emission tomography (PET) (1,2) is an important technological step forward in this regard. Despite extensive use in other medical disciplines (neurology and cardiology) (3-5), PET's application to pulmonary disorders is just beginning, but already it appears extremely promising.

TECHNOLOGY AND METHODOLOGY

Conventional nuclear medicine imaging depends upon the external detection of radiation produced by radionuclides which emit single gamma photons. The quantitative interpretation of such data, however, is limited by shortcomings common to single photon detection systems. The most troublesome is the variable degree of attenuation (i.e., absorbed or scattered radiation) that occur between the site of the decay event and the detector. This attentuation is a complex function of photon energy, nature of the tissue, and the distance between the event and the detector. Although single photon emission computed tomography (SPECT) (6,7) improves the regional *localization* of where detected events have occurred, it does not add substantially to the quantitative accuracy of the regional radioactivity measurement.

The unique property of some nuclides to decay by positron emission, together with

a novel approach to radiation detection (coincidence counting) has provided an approach that minimizes the problem of variable attenuation (8-10). After sufficient numbers of coincidence events have been detected and recorded, a distribution of radioactivity can be reconstructed from the data, and displayed tomographically using mathematical approaches identical to those adopted for conventional x-ray computed tomography. The *physiologic meaning* of this spatial distribution, however, requires an appropriate mathematical model that accurately describes the physiologic process in question. Thus, positron emission tomography (PET) requires 3 basic components to produce an image which is a valid, quantitative representation of some physiologic process: 1) a radiopharmaceutical labeled with a positron-emitting nuclide, 2) a device that accurately measures the regional radioactivity emitted by this radionuclide, and 3) a mathematical model that converts the quantitative measurement of regional radioactivity into an estimate of some physiologic variable.

Positron-emitting radiopharmaceuticals

All the nuclides used in PET studies decay by the same process: positron emission (1). As a result, a particle with the mass of an electron but a positive (instead of negative) charge is emitted from the isotope's nucleus. The positron travels 2-5mm before interacting with an electron (the actual distance is related to the energy of the emitted positron). The result of this interaction is the annihilation of each particle and the consequent emission of two 511 keV photons traveling nearly 180° apart from one another (the slight difference being due to the angular momentum of the positron versus the electron). These two photons easily penetrate body tissue and accordingly they can be recorded by detectors placed on opposite sides of the body.

Positron-emitting radionuclides commonly used in PET studies include isotopes carbon-11, nitrogen-13, and oxygen-15, elements which are naturally present in the body (11-14). Although the short half-life (2-21 min) of these isotopes often necessitates "on-site" cyclotron production, it also provides a unique opportunity to perform sequential studies without excessive absorbed radiation. The diversity of radiopharmaceuticals which can be prepared with these three nuclides is primarily limited by time constraints in chemical synthesis imposed by the short half-life of the particular nuclide.

Gallium-68 has also been used for pulmonary studies *(see below)*. It differs from the other nuclides in two unique respects: 1) it is a metallic element, not natural to the body, and 2) it is generator-, not cyclotron-produced.

Positron-emission detection systems

Photons emitted after annihilation of the positron with an electron may be recorded by detectors placed 180° apart from one another *(Fig. 1)* (8,9). Localization of this event in space is achieved by connecting each detector pair electronically and recording the event only if each detector registers the event within a brief timing "window" (typically < 10-20 nanosec). The value for this window varies with the detector material. Each "coincidence" detection signifies that "annihilation" occurred at some point between the detector pair. Single, unpaired events registered at either detector are not recorded. This electronic coincidence provides collimation which is typically 100 times more efficient than that provided by lead shielding in conventional single photon detection systems (2). Furthermore, uniform spatial resolution is achieved since the sensitivity of the detectors is unrelated to the position of the radiation source between them.

By chance, single photons from different annihilation events may also be registered within the timing window at each detector in the pair *(Fig. 1)*. The proportion of such "random" coincidences to "true" coincidences is a function of both the duration of the timing window and the total amount of activity. Including these "randoms" in the data used to eventually construct the PET image degrades the accuracy of the regional activity measurements (i.e., decreases the signal-to-noise ratio). Newer generation detection systems are capable of

actually recording the time delay between the two photons arriving at the detector pair (so-called "time of flight" information) (15). This additional data helps locate where the event occurred between the detectors, and thus reduces the statistical noise that such random coincidence events contribute to the processed image.

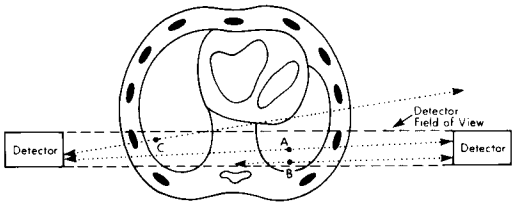

Fig. 1. Schematic representation of cross-section through the chest. Solid circles represent site of annihilation events due to interaction of a positron with an electron and arrows represent emitted gamma photons. Photons arriving from event A are detected within an allowable "coincidence window" and this data ("true" coincidence) is then used in late image reconstruction. Events B (one attenuated photon) and C (single photon detection only) are not recorded by the detector pair, and thus are excluded from use during image reconstruction. However, if events B and C emit photons and by chance arrive at the detector pair within the allowable coincidence window, they could be used for image reconstruction even though they represent more than one event ("random" coincidence). This capability is true even if individual events occur outside the detector field of view.

The PET imaging device itself consists of multiple detector pairs, usually arranged in circular fashion. The number of rings of such detectors determines the number of tomographic slices, and detector dimensions determine slice width, detector resolution, and absorption efficiency. All recorded true coincidence events for each detector pair are used to create the tomographic image, using the same filtered back projection technique employed in conventional x-ray computer tomography. The final result is a reconstructed image which is an accurate quantitative representation of regional tissue radioactivity. Devices currently in use at Washington University include the PETT-VI and the SUPER PETT-I scanners (16-18). PETT-VI consists of 4 rings of 72 detectors each. The field-of-view diameter is 27cm. Direct plane and cross plane coincidence lines are recorded to yield 7 simultaneous slices with a center-to-center spacing of 1.44cm. Cesium fluoride crystals are used as the scintillation detectors. In the "low-resolution" mode, the in-plane physical resolution is 1.17cm (full width, half maximum) at the center. Slice thickness is 1.39cm for direct slices and 0.97cm for cross slices. Design characteristics for SUPER-PETT I have also been reported (18).

Mathematical models used in PET studies

Although some information may be obtained by analyzing the relative distribution of radioactivity within a PET image, more useful information is achieved by converting this activity data into units of the physiologic variable of interest. This conversion requires a mathematical model. Such models may be mathematically simple (e.g., as used in the measurement of regional blood volume) (19) or of considerable complexity (as in the measurement of tissue glucose metabolism) (20). Nonetheless, the data ultimately obtained is only as accurate as the model used in its calculation. This feature holds true regardless of how good PET itself is for making accurate measurements of regional tissue radioactivity. The power of PET techniques therefore depends on the accuracy with which the model represents the relevant physiology. Without this model, PET is simply another form of tomographic imaging; with it, however, PET becomes a powerful analytical tool for studying *in vivo* physiology repetitively and noninvasively.

PULMONARY MEASUREMENTS WITH PET

General considerations

Three problems are of special importance in analyzing pulmonary PET data. The first is partial-volume averaging (21): the measurement of radioactivity in any given region of a reconstructed PET image represents not only activity within that re-

gion, but also some portion of the activity within surrounding regions as well. The magnitude of this effect depends on positron range, scanner resolution, and the true distribution of the radioactivity. The effect is greatest when heterogeneity of regional tissue activity is broadest. With respect to lung studies, the partial-volume averaging effect is likely to be most important for regions near the heart, large vessels (such as the aorta or vena cava), or chest wall.

A related problem is that created by respiratory motion. In effect, the movement of structures with heterogeneous activity in and out of a region of interest during a scan creates artifact comparable to partial-volume averaging. This problem is greatest for scans of long duration, taken during ventilation with large tidal volumes, in areas where tissue activity is most heterogeneous. Although preliminary data seem to indicate that this issue is manageable in experimental studies (19), its importance in a more general sense is not yet known. Newer generation scanners which allow respiratory gating may resolve this problem.

Finally, a potential shortcoming unique to pulmonary studies is that of data expression (19,22,23). PET data are expressed in terms of lung volume (usually ml/lung). Thus the value of PET measurement may change because either a true change in the variable being studied occurred, or because a change in regional inflation (i.e., lung volume) developed. Although no simple solution has been developed, interpretation is often facilitated by normalizing the PET data (or at least comparing it) to other regional data obtained by PET (e.g., tissue density to blood volume) (19,22,24).

Pulmonary blood flow

Studying the distribution of pulmonary

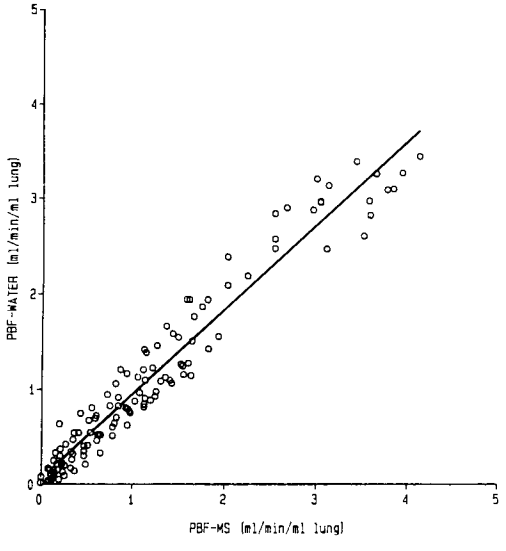

Fig. 2. Correlation plot of regionally measured pulmonary blood flow using Ga-68 microspheres (PBF-MS) versus blood flow measured with the 0-15 water technique (PBF-water). Data are from 126 regions obtained in 12 dogs. The regression equation for the line shown is PBF-water = 0.89 (PBF-MS) + 0.56 (r = 0.972). When considering only points below 3 ml/min/ml lung, the slope of the regression (not shown) improves considerably (PBF-water = 0.98 (PBF-MS) − 0.14, r = 0.96.

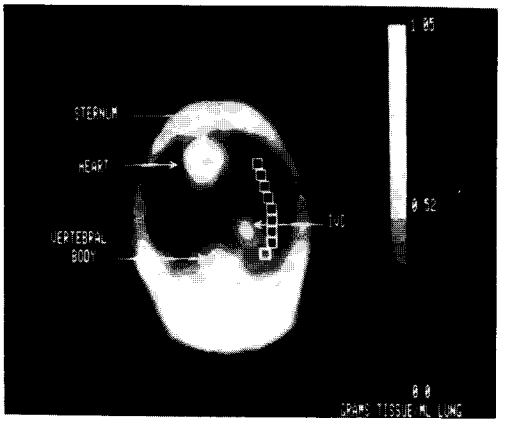

Fig. 3. Single slice image of a dog chest from a transmission scan used to correct subsequent emission scans for undetected radiation lost to absorption or scatter. The image is analogous to conventional x-ray computed tomographic imaging, except for poorer spatial resolution and less distinction between bone and soft tissue. Attenuation values assigned to each pixel have been scaled to units of density (gm/ml) after establishing a linear correlation between the known densities of a variety of phantoms and the arbitrary attenuation numbers obtained during scanning. The slice is from a position approximately 2cm above the diaphragm. The animal was supine and the right side of the image is the right side of the animal. IVC = inferior vena cava.

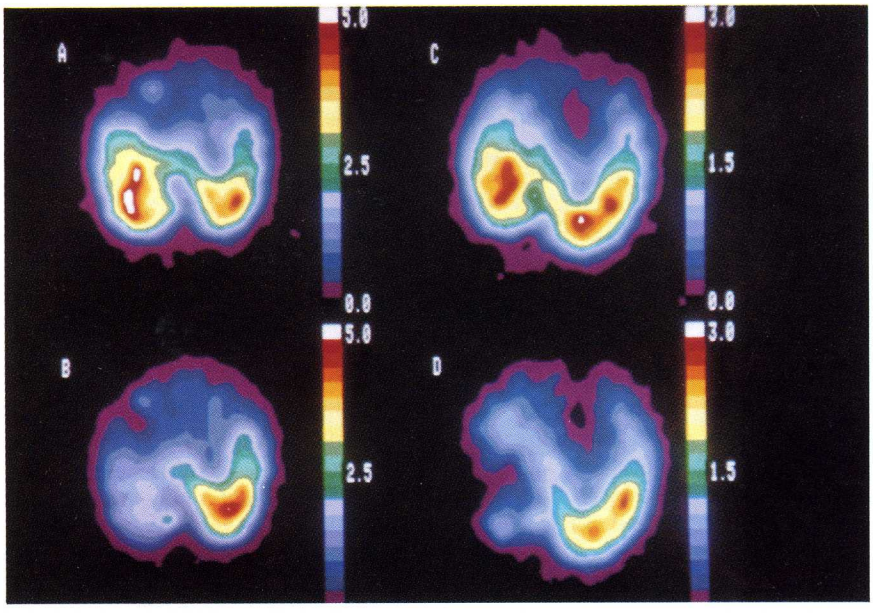

Fig. 4. Left side: Transverse tomographic slices of pulmonary blood flow (PBF) from one animal before (A) and after (B) ventilating the left lower lobe with 100% nitrogen. Scales at the right of each figure represent PBF in ml/min/ml lung. Note the reduction of blood flow in the hypoxic left lung with little or no change in the normoxic lung. Right side: Similar tomographic slices of PBF from another animal before (C) and after (D) oleic acid administration into the left lower lobe. Once again PBF decreases in the affected lung with little or no change on the unaffected side.

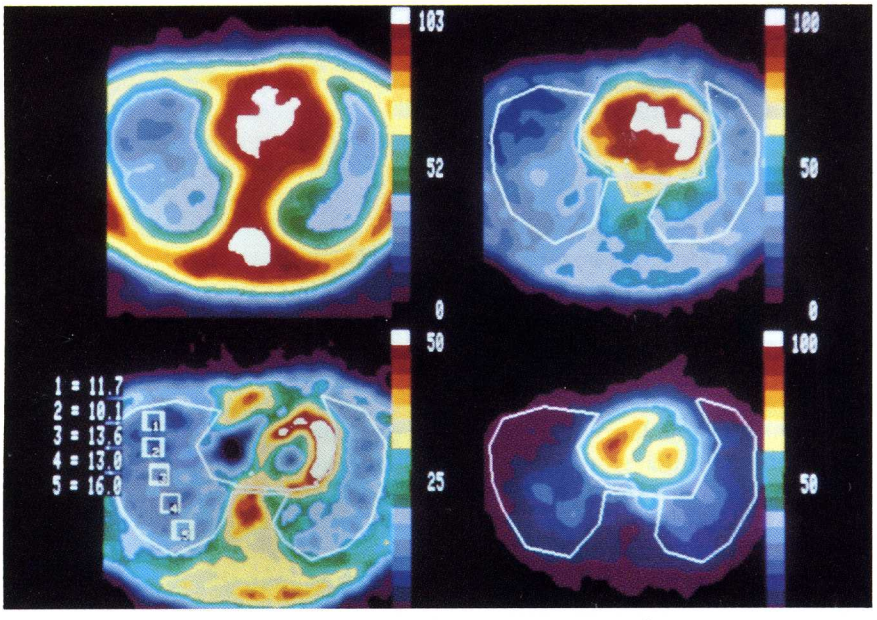

Fig. 5. Transverse tomographic images from one normal human subject showing topographic distribution of density (upper left), total lung water (upper right), intravascular lung water (lower right) and extravascular lung water (lower left). Scale of density in gm/100ml lung. All other scales in ml H_2O/100ml lung. Values for extravascular lung water in selected regions are also shown in the lower left panel. Orientation of the image is reversed from Fig. *3, i.e., right side of the image is left side of the subject.*

blood flow (PBF) during acute respiratory failure is difficult because most techniques are not quantitative, repeatable, or regional. The traditional use of radiolabeled microspheres (or macroaggregates) *in vivo* is probably the "gold standard" for determining regional PBF, but accurate quantitative regional information is obtained only by removing the lung and processing individual tissue samples, an approach which is cumbersome experimentally and unsuitable clinically.

We have described an alternative approach using PET and 0-15 labeled water. The method is based on autoradiography as originally described by Kety and colleagues (25,26), and modified for PET by Herscovitch and Raichle (27,28). PET data are interpreted with a one-compartment mathematical model in which the tracer is assumed to enter lung tissue via incoming blood, to distribute freely through vascular and extravascular areas, and to exit at a concentration equal to the tissue concentration divided by the tissue-blood equilibrium partition co-efficient for the tracer. The measurement itself requires a 15 second PET scan obtained during a 20 second constant infusion of 0-15 water into a central vein, followed by a 5 min scan obtained 4 min after isotope administration. The latter scan is used to estimate the regional tissue-blood partition coefficient for water (22).

The initial distribution of the 0-15 water tracer is directly related to regional PBF, but actual quantitation also requires measurement of the time-activity curve of blood perfusing the lung (22). This is obtained by simultaneous sampling of pulmonary arterial blood during the PET scan via an appropriately positioned indwelling catheter.

When compared to standard microsphere methods, this technique for measuring regional PBF is accurate over a reasonable range of blood flows *(Fig. 2)*. Reproducibility is also acceptable (coefficient of variation <14% for regions approximately 0.9ml in volume). Besides accurate regional PBF measurements *in vivo*, this approach also allows rapid repeated measurements because the half-life of 0-15 is short (2.05 min). PBF measurements are made before and after a given intervention, or temporally close to some other measurement made with PET (e.g., lung water).

Several important limitations of this technique are apparent, however. First, a large amount of data, representing tissue activity measurements, must be collected over a brief period of time. Therefore, the technique is limited to scanners capable of accurately recording data at very high counting rates. Second, quantitation at present depends on blood sampling of pulmonary arterial blood, making the technique less desirable as a clinical tool. Third, the relationship between PBF and measurements of regional tissue activity is non-linear at blood flows much above normal (22). At high blood flows, small errors in the tissue activity measurement result in relatively large changes in calculated PBF. Fourth, the calculation of PBF is strongly influenced by the local value for the partition coefficient (22), so that errors are greatest in low-density regions of the lung. Thus, the PET measurement of regional PBF, based on the autoradiographic approach with 0-15 labeled water, is most likely misleading in low-density regions with high blood flow. Nonetheless, the technique theoretically is ideal for studying lung injury, since much of the pathophysiologic change of lung injury occurs in high-density areas of lung with regional decreases in PBF. On the other hand, the technique is less useful with high pulmonary blood flows as in exercise physiology, although in this situation it may be possible to measure PBF with microspheres labeled with a positron-emitter. PBF has already been measured by PET in several studies of regional hypoxic pulmonary vasoconstriction and acute lung injury (29,30) and examples of scans from such experiments are shown in *Figs. 3 and 4*. Because this technique still requires sampling of pulmonary arterial blood, it is not yet readily applicable to human studies, but suggested modification in this regard are underway (22).

Extravascular lung water (EVLW)

Measurement of EVLW is feasible with PET by subtracting the intravascular water

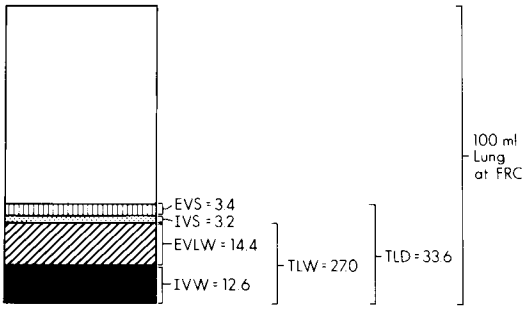

Fig. 6. Lung compartments as defined by mean PET measurements obtained in 6 dogs. EVS = extravascular space; IVS = intravascular space; EVLW = extravascular lung water; IVW = intravascular water; TLW = total lung water; TLD = total lung density; FRC = functional residual capacity.

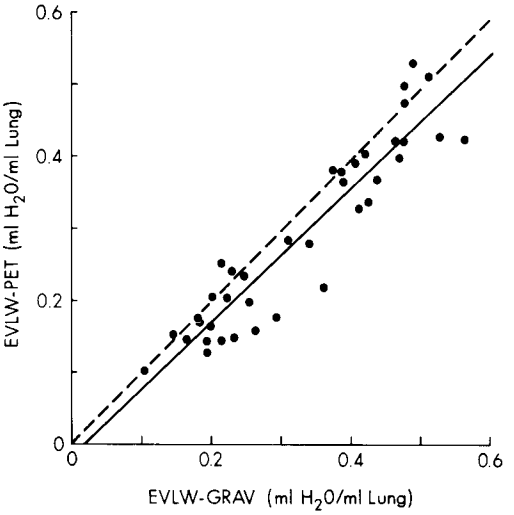

Fig. 7. Correlation of regional EVLW determined by PET to EVLW determined by gravimetric techniques, as explained in reference 26. The regression equation for the solid line is EVLW-PET = 0.93 (EVLW-grav) − 0.02 for 38 samples obtained from 8 dogs (r = 0.93).

content of a region (IVW) from the total lung water content of that same region (TLW) (19). The intravascular component is measured by scanning the subject at least 2 min after an inhalation of ^{15}O-labeled carbon monoxide, a gas that avidly binds to hemoglobin. IVW is calculated by referencing the radioactivity in a given lung region to activity in blood samples taken during the scan. A similar procedure is used to measure TLW, except the scan is obtained after equilibrium of a bolus infusion of 0-15 labeled water. This measurement may be done at the same time the partition coefficient is determined during regional PBF measurements with PET (19,22). The extravascular water content of a region (EVLW), then, simply reduces to subtraction of IVW from TLW *(Fig. 5)*. Alternatively, a constant infusion of ^{15}O-water (31), or ^{11}C- instead of ^{15}O-labeled CO (24), or density instead of TLW measurements have also been utilized (24). If density, water and blood volume measurements are combined, mean values for the various lung compartments can be defined *(Fig. 6)*. Recent studies in whole animals suggest that PET provides measurements of EVLW with acceptable accuracy in both normal and edematous lung *(Figs. 6 and 7)* and is sensitive to small changes in EVLW after physiologic intervention (23). To date, values obtained in humans are comparable to those obtained in experimental animals (32-35).

Pulmonary vascular permeability (PVP)

Although PET may measure accumulation of EVLW during pulmonary edema, the pathogenesis of this edema requires further clarification. Pulmonary edema is usually classified as either "cardiogenic" or "noncardiogenic". Often, the phenomenon of "increased permeability" pulmonary edema is made by inference; when pulmonary edema develops in the setting of normal hydrostatic pressure (estimated from pulmonary artery wedge pressure) its pathogenesis is ascribed to a non-cardiogenic origin. This distinction, however, ignores that pulmonary edema may arise simultaneously from both cardiac and non-cardiac sources, that therapy itself may alter hydrostatic pressure, or that the "permeability defect" encompasses a wide range of severity that is estimable only by direct measurement.

Recently, we developed a method of evaluating PVP by adapting a technique of Gorin et al (36) for measuring the flux of a radiolabeled protein across the pulmonary endothelium by external radiation detection. Gorin et al validated this technique

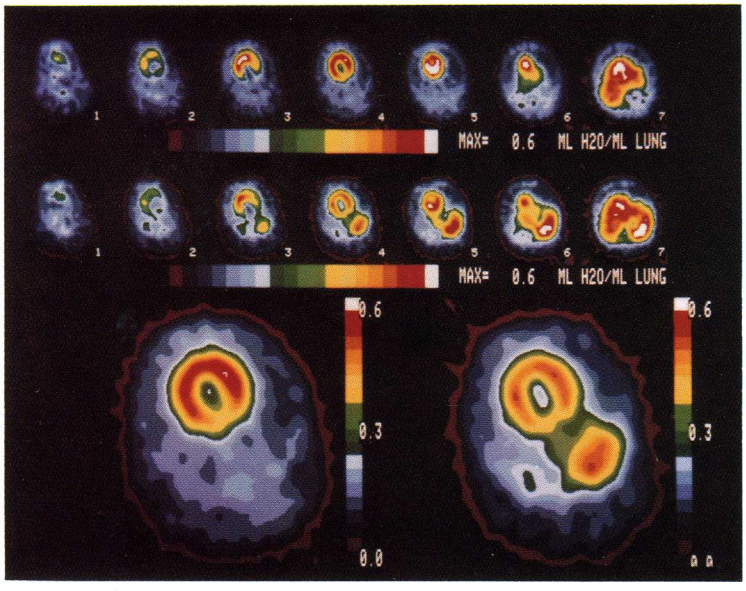

Fig. 8. Upper half: EVLW images on all 7 slices before (first row) and after (second row) oleic acid injected into the right lower lobe. The orientation of each image is the same as in Fig. 3. *Lower half: Enlargements of slice 4 showing regional increases in EVLW in the right lower lobe. The image in the lower left was obtained prior to and that in the lower right after oleic acid. EVLW in each scan slice has been scaled to a maximum (MAX) value of 0.6ml water/ml lung. The circular object in the upper portion of each scan slice is a transverse section through the heart.*

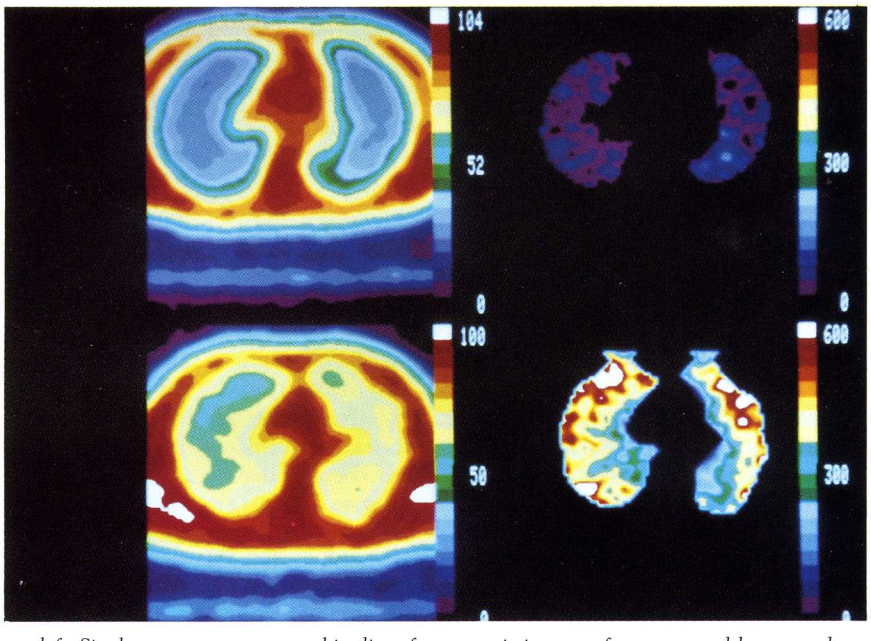

Fig. 9. Upper left: Single transverse tomographic slice of a transmission scan from a normal human volunteer. Color scale and orientation as in Fig. 5. *Upper right: PTCER image obtained in the same slice of the normal volunteer. Color scale in units of 10^{-4} min^{-1}. Lower left: Transmission image from a patient with ARDS. Note the increase in tissue density, compared with the normal volunteer. Lower right: PTCER image obtained in the same slice of the ARDS patient. Note the marked increase in PTCER compared with the normal volunteer.*

by comparing the calculated index of vascular permeability with direct measurements of protein flux into lung lymph in sheep; later on, the method was adapted to humans (37).

With PET adaptation (38), Ga-68 citrate is administered intravenously. The Ga-68 rapidly dissociates from the citrate and binds tightly to native transferrin. Rapid equilibration within the intravascular blood pool is followed by a slow egress of this protein macromolecule from blood into the extravascular space, including that of the lung. The time required for equilibration between intra- and extravascular spaces depends on both the local capillary endothelial permeability to that protein, and the surface area available for exchange. If both the plasma time-activity curve (from direct blood sampling) and the local extravascular tissue time-activity curve (from PET scanning) are known, a protein permeability-surface area product can be calculated. Gorin termed this rate constant the pulmonary transvascular capillary escape rate (PTCER), after normalizing it for regional values of pulmonary plasma volume. The purpose of this normalization is to adjust the measurement for regional differences in surface area available for protein transport.

In experimental animals, after oleic acid induced injury limited to the left lower lobe, we estimated PTCER to be 49 ± 18 in normal lung tissue and 485 ± 114 10^{-4} min^{-1} in injured lung, findings that persisted for 4 hrs. Values recently obtained in normal human subjects and in patients with adult respiratory distress syndrome showed similar differences between normal and abnormal lung parenchyma *(Fig. 9)*. Although diffuse infiltrates persisted radiographically, and the patients still required mechanical ventilatory support with positive end-expiratory pressure, notable clinical improvement had occurred at the time of the PET study. Nevertheless, PTCER was still abnormally elevated, indicating how much more needs to be learned about the natural history of the permeability defect after lung injury.

Other pulmonary measurements

PET has also been used to measure regional ventilation and regional ventilation-to-perfusion ratios (39-46). An exciting possibility is that PET may be able to evaluate pulmonary metabolism non-invasively (47). Lung studies may include glucose metabolism, receptor physiology, and lung amine uptake and clearance function. The techniques for performing these measurements are still only in the earliest stage of development, validation, and application.

ACKNOWLEDGEMENT

This work was supported in part by NIH Grant HL32815 and Department of Energy Grant DE-AC02-77EV04318.

REFERENCES

1. Ter-Pogossian, MM, ME Raichle, BE Sobel: Positron emission tomography. Sci. Amer. 243 (1980), 171-181.
2. Ter-Pogossian, MM: Special characteristics and potential for dynamic function studies with PET. Semin. Nucl. Med. 21 (1981), 13-23.
3. Phelps, ME: Positron computed tomography for studies of myocardial and cerebral function. Ann. Intern. Med. 98 (1983), 339-359.
4. Powers, WJ, ME Raichle: Positron emission tomography and its application to the study of cerebrovascular disease in man. Stroke 16 (1985), 361-376.
5. Geltmann, EM, BE Sobel: Cardiac positron tomography. Chest 83 (1983), 553-557.
6. LeJeune, JJ, J Maublant, M Lahellec, et al: Emission computed tomography vs. perfusion scanning in lung disease. Eur. J. Nucl. Med. 7 (1982), 171-173.
7. Biersack, HJ, H Altland, R Knopp et al: Single photon emission computer tomography of the lung: Preliminary results. Eur. J. Nucl. Med. 7 (1982), 166-170.
8. Phelps, ME, Hoffman, EJ, NA Mullani, et al: Application of annihilation coincidence detection to transaxial reconstruction tomography. J. Nucl. Med. 16 (1975), 210-223.
9. Ter-Pogossian, MM: Basic principles of computed axial tomography. Semin. Nucl, Med. 7 (1977), 109-127.
10. Chesler, DA, C Hales, DJ Hnatowich, et al: Three-dimensional reconstruction of lung perfusion image with positron detection. J. Nucl. Med. 16 (1975), 80-82.
11. Welch, MJ, MM Ter-pogossian: Preparation

of short-lived radioactive gases for medical studies. Radiation Research 36 (1968), 580-587.
12. Welch, MJ: Choice and preparation of radioactive gases. Prog. Nucl. Med. 3 (1973), 37-48.
13. Clark, JC, PD Buckingham: *Short-Lived Radioactive Gases for Clinical Use*. Butterworths, London, 1975.
14. Buckingham, PD, JC Clark: Nitrogen-13 solutions for research studies in pulmonary physiology. Int. J. Appl. Rad. Isot. 23 (1972), 5-8.
15. Ter-Pogossian, MM, NA Mullani, DC Ficke, et al: Photon time-of-flight-assisted positron emission tomography. J. Comp. Asst. Tomogr. 5 (1981), 227-239.
16. Yamamoto, MM, DC Ficke, MM Ter-Pogossian: Performance study of PETT VI, a positron computed tomography with 288 cesium fluoride detectors. IEEE Trans. Nucl. Sci. NS-29 (1982), 529-533.
17. Ter-Pogossian, MM, DC Ficke, JT Hood, et al: PETT-VI: A positron emission tomography utilizing cesium fluoride scintillation detectors. J. Comput. Asst. Tomogr. 6 (1982), 125-133.
18. Ter-Pogossian, MM, DC Ficke, M Yamamoto, et al: Design characteristics and preliminary testing of Super-PETT I, a positron emission tomography utilizing photon time-of-flight information (TOF PET). IEEE Workshop on Time-of-Flight Tomography, May, 1982, pp. 37-41.
19. Schuster, DP, MA Mintun, MA Greene, et al: Regional lung water and hematocrit determined by positron emission tomography. J. Appl. Physiol. 59 (1985), 860-868.
20. Sokoloff, L: Application of quantitative autoradiography to the measurement of biochemical processes *in vivo*. In: *Positron Emission Tomography*. Reivich, M, A Alavi (Eds.), Alan R. Liss, Inc., New York, 1985, pp. 1-42.
21. Hoffman, EJ, S Huang, ME Phelps: Quantitation in positron emission computed tomography: 1. Effects of object size. J. Comp. Assist. Tomogr. 3 (1979), 299-308.
22. Mintun, MA, MM Ter-Pogossian, MA Greene, et al: Quantitative measurement of regional pulmonary blood flow with positron emission tomography. J. Appl. Physiol. 60 (1986), 317-326.
23. Schuster, DP, GF Marklin, MA Mintun: Regional changes in extravascular lung water detected by positron emission tomography. J. Appl. Physiol. 60 (1986), 1170-1178.
24. Rhodes, CG, P Wollmer, F Fazio, et al: Quantitative measurement of regional extravascular lung density using positron emission and transmission tomography. J. Comp. Assist. Tomogr. 5 (1981), 783-791.
25. Kety, SS: Measurement of local blood flow by the exchange of an inert, diffusible substance. Methods Med. Res. 8 (1960), 228-236.
26. Kety, SS: The theory and application of the exchange of inert gas at the lung and tissues. Pharmacol. Rev. 3 (1951), 1-4.
27. Herscovitch, P, J Markham, ME Raichle: Brain blood flow measured with intravenous $H_2{}^{15}O$. I. Theory and error analysis. J. Nucl. Med. 24 (1983), 782-789.
28. Raichle, ME, MRW Martin, P Herscovitch et al: Brain blood flow measured with intravenous $H_2{}^{15}O$. II. Implementation and validation. J. Nucl. Med. 24 (1983), 790-798.
29. Schuster, DP, GF Marklin: The effects of alveolar hypoxia or lung injury on regional pulmonary blood flow measured by positron emission tomography. Am. Rev. Respir. Dis. 135 (1986), 1037-1042.
30. Dennis, DR, DP Schuster: Diethylcarbamazine does not attenuate hypoxic pulmonary vasoconstriction in the dog. Am. Rev. Respir. Dis. 133 (1986), 398A.
31. Meyer, GJ, O Schober, C Bossaller, et al: Quantification of regional extravascular lung water in dogs with positron emission tomography, using constant infusion of ^{15}O-labeled water. Eur. J. Nucl. Med. 9 (1984), 220-228.
32. Wollmer, P, CG Rhodes, RM Allan, et al: Regional extravascular lung density and fractional blood volume in patients with chronic pulmonary venous hypertension. Clin. Phys. 3 (1983), 241-256.
33. Schober, OH, GJ Meyer, C Bossaller, et al: Quantitative determination of extravascular lung water and regional blood volume in congestive heart failure. Eur. J. Nucl. Med. 10 (1985), 17-24.
34. Wollmer, P, A Rozkovec, CG Rhodes, et al: Regional pulmonary blood volume in patients with abnormal blood pressure or flow in the pulmonary circulation. Eur. Heart J. 5 (1984), 924-931.
35. Wollmer, P, CG Rhodes, JMB Hughes: Regional extravascular density and fractional blood volume of the lung in interstitial disease. Thorax 39 (1984), 286-293.
36. Gorin, AB, WJ Weidner, RH Demling, et al: Non-invasive measurement of pulmonary transvascular protein flux in sheep. J. Appl. Physiol. 45 (1978), 225-233.

37. Gorin, AB, J Kohler, G DeNardo: Noninvasive measurement of pulmonary transvascular protein flux in normal man. J. Clin. Invest. 66 (1980), 869-877.
38. Dennis, DR, MA Mintun, DP Schuster: Measurement of pulmonary vascular permeability by positron emission tomography. Am. Rev. Respir. Dis. 133 (1986), A20.
39. Greene, R, CA Burnham: Positron-camera studies of regional ventilation with ^{13}N. J. Nucl. Med. 13 (1972), 433-434.
40. Greene, R, B Hoop, H Kazemi: Use of ^{13}N in studies of airway closure and regional ventilation. J. Nucl. Med. 12 (1971) 719-723.
41. Senda, M, K Murata, H Itoh, et al: Quantitative evaluation of regional pulmonary ventilation using PET and N-13 nitrogen gas. J. Nucl. Med. 27 (1986), 268-273.
42. Brudin, LH, CG Rhodes, SO Valind, et al: Topographic relationships between ventilation, ventilation to perfusion ratio, and extravascular density in patients with emphysema and chronic bronchitis using positron emission tomography (PET). Am. Rev. Respir. Dis. 131 (1985), A67.
43. Valind, SO, P Wollmer, CG Rhodes: Application of positron emission tomography in the lung. In *Positron Emission Tomography*, Reivich, M, A Alavi (Eds.), Alan R. Liss, Inc., New York, 1985, pp. 387-412.
44. Valind, SO, CG Rhodes, JC Clark, et al: Quantitative measurements of regional ventilation using positron computed tomography and a short-lived inert gas-neon-19. Nucl. Med. Commun. 4 (1983), 149.
45. Brudin, LH, Rhodes, CG, SO Valind, et al: Regional ventilation to perfusion ratio and ventilation in asthmatics using positron emission tomography (PET). Am. Rev. Respir. Dis. 131 (1985), A283.
46. Brudin, LH, Rhodes, CG, Valind, SO, et al: Topographic relationships between ventilation, ventilation to perfusion ratio, alveolar volume, and extravascular density in man using positron emission tomography (PET). Am. Rev. Respir. Dis. 131 (1985), A313.
47. Rhodes, CG, SO Valind, T Suzuki, et al: Regional measurement of pulmonary glucose utilization rate and distribution volume in man. Am. Rev. Respir. Dis. 129 (1984), 309A.

Daniel Schuster, M.D.
Department of Internal Medicine
Washington University School of Medicine
Box 8052
660 South Euclid Avenue
St. Louis, MO 63110